



Contents lists available at ScienceDirect

Journal of King Saud University – Science

journal homepage: [www.sciencedirect.com](http://www.sciencedirect.com)

## Original article

## Investigating the effect of food additive dye “tartrazine” on BLG fibrillation under in-vitro condition. A biophysical and molecular docking study

Nasser Abdulatif Al-Shabib <sup>a,\*</sup>, Javed Masood Khan <sup>a,\*</sup>, Ajamaluddin Malik <sup>b</sup>, Md Tabish Rehman <sup>c</sup>, Mohamed F. AlAjmi <sup>c</sup>, Fohad Mabood Husain <sup>a</sup>, Aqeel Ahmad <sup>d</sup>, Priyankar Sen <sup>e</sup><sup>a</sup> Department of Food Science and Nutrition, Faculty of Food and Agricultural Sciences, King Saud University, 2460, Riyadh 11451, Saudi Arabia<sup>b</sup> Protein Research Chair, Department of Biochemistry, College of Science, King Saud University, Riyadh, Saudi Arabia<sup>c</sup> Department of Pharmacognosy, College of Pharmacy, King Saud University, Riyadh 11451, Saudi Arabia<sup>d</sup> Department of Medical Biochemistry, College of Medicine, Shaqra University, Shaqra 11961, Saudi Arabia<sup>e</sup> Centre for Bioseparation Technology, Vellore Institute of Technology, Vellore 632014, India

## ARTICLE INFO

## Article history:

Received 28 August 2019

Revised 17 October 2019

Accepted 11 February 2020

Available online 20 February 2020

## Keywords:

Tartrazine

Beta-lactoglobulin

Food additive dye

Amyloid fibril

pH

## ABSTRACT

Tartrazine (Tz) is a yellow food color dye that is used in a range of foods to make them more appealing and attractive. However, very limited information is there about its interaction with macromolecules, like different proteins that are components of the food products. In this work the bovine beta-lactoglobulin (BLG) aggregation stimulating properties of Tz have been studied at pH 2.0. Spectroscopic, microscopic and molecular docking have been used to characterize the aggregation inducing property of Tz in BLG protein at pH 2.0. The spectroscopic techniques i.e., turbidity and RLS measurements showed that the 0.1–10.0 mM of Tz induces aggregation in BLG at pH 2.0. The aggregates were found to have well defined amyloid-like morphology as observed by CD and TEM. The amyloid fibrils were found long, straight and unbranched. Molecular docking results ascertained that Tz binds at the hydrophobic cavity and interact with the key amino acid residues involved in the interaction with different ligands. The spectroscopic, microscopic and computational results support that the electrostatic, as well as hydrophobic interactions, played a very important role in Tz-induced BLG fibrillation.

© 2020 The Author(s). Published by Elsevier B.V. on behalf of King Saud University. This is an open access article under the CC BY-NC-ND license (<http://creativecommons.org/licenses/by-nc-nd/4.0/>).

## 1. Introduction

Artificial azo dyes are playing a very important role in appearance and enhancement of the quality of foods. Azo dyes are making products more attractive to the consumers particularly children (Hofer and Jenewein, 1997). Azo dyes are in use for a long time in food industry worldwide, but its uses are controversial in the light of its adverse effects on health (Eman et al., 2000). Azo dyes contain at least one group N=N in the molecule with two to three aromatic rings. The European Union has permitted some azo dyes to be used in food products such as the tartrazine (Tz) (E102); Quinoline Yellow (E104) and Sunset Yellow (E110). Tz is an

orange-colored, water-soluble dye with inclusive applications in food industries, cosmetics, textiles, drugs, and pharmaceuticals (Merinas-Amo et al., 2019). Tz is anionic molecule having benzene ring also shown in Fig. 1A. Food Additives (JECFA) reported the data of more than 300 studies on laboratory animals and clinical trials on human beings on toxicological concern in 1964. From the report it was found that Tz has no cancer causing potential while have little adverse effect on reproduction and development (Collins et al., 1990, Tanaka et al., 2008). Thus, intake of low concentrations of Tz doesn't cause any genotoxicity in humans (Poul et al., 2009). It will be interesting to check the effects of Tz on proteins found in milk.

Several molecules like surfactants, natural dyes (curcumin) and glycosaminoglycan induces amyloid-like aggregates in several proteins (Abelein et al., 2013; Khan et al., 2018a,b). The protein aggregates are sometimes toxic and causes several neurodegenerative diseases such as Alzheimer's disease, Parkinson's disease, etc. and non-neurodegenerative diseases (type 2 diabetes, systemic amyloidosis etc) (Blancas-Mejía and Ramirez-Alvarado, 2013; Wawer et al., 2018). These proteins are not necessarily belongs to the same

\* Corresponding authors.

Peer review under responsibility of King Saud University.



Production and hosting by Elsevier

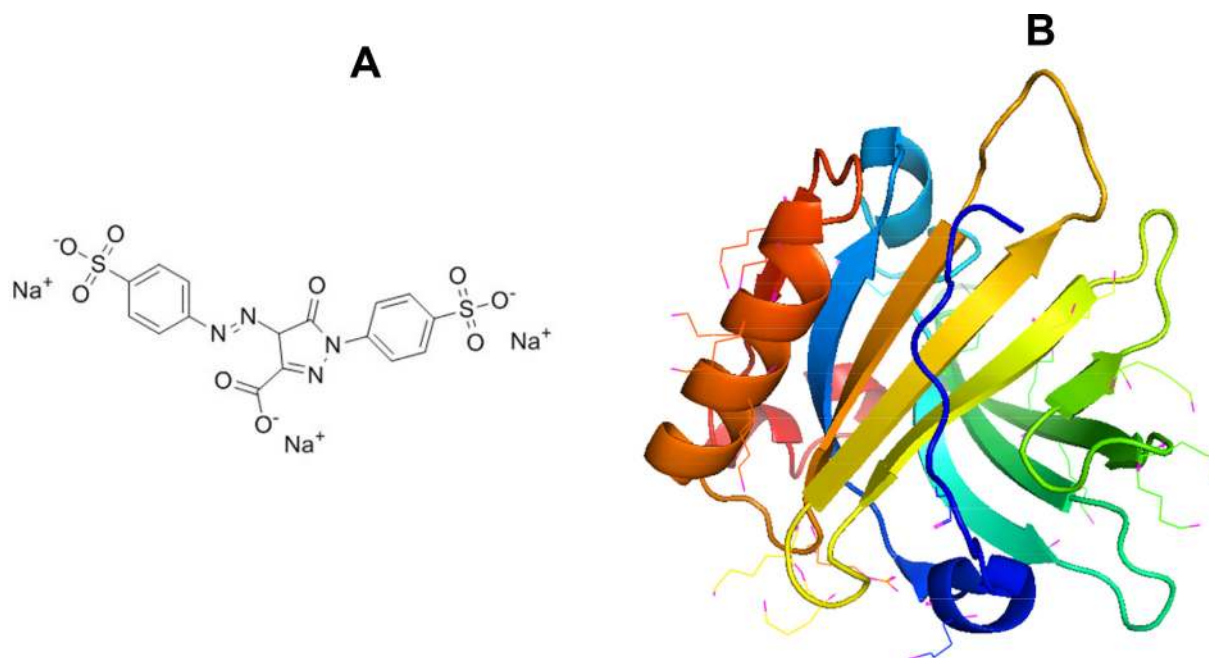


**Fig 1.** (A) Molecular structure of tartrazine dye (Tz) and (B) Crystal structure of BLG (PDB ID: 3NPO).

family, in fact most of them are dissimilar in structure and function. These protein aggregates are mainly made up of ordered cross  $\beta$  structures, called amyloid fibril (Biancalana and Koide, 2010). Amyloid fibrils are straight, unbranched of 70–120 Å in diameter and of indeterminate length confirmed by electron microscopy measurements (Shirahama and Cohen, 1996). Amyloid fibril formation follows nucleation dependent pathways (Chiti and Dobson, 2017). It is reported that the amyloid fibril can form both *in-vivo* and *in-vitro* (Bieler et al., 2005). Several factors (temperature, pH, denaturant, surfactant, and food dyes) are now known to accelerate amyloid fibril formation in proteins (Chiti et al., 1999; Al-Shabib et al., 2017; Khan et al., 2016a,b). Among the food additive dyes, Tz and allura red are known to accelerate amyloid fibril formation (Al-Shabib et al., 2017). Understanding the role of Tz into amyloid fibrillation of bovine beta lactoglobulin milk protein is important.

Bovine beta lactoglobulin (BLG) is important globular whey proteins containing two disulfide bonds at the position of C106–C119 and C66–C160 and one free cysteine (C121) shown in Fig. 1B (Mecherfi et al., 2019). BLG exists mainly as a dimer at room temperature and at physiological pH. The monomer units of BLG associate non-covalently and dissociate into its monomers (MW = 18.3 kDa) at higher temperatures (Verheul et al., 1999). The aggregation of BLG is studied more than any other whey protein. The majority of the aggregation studies of BLG have been conducted at denaturing conditions like extremes in pH or temperature (Schmitt et al., 2007), or by several intrinsic (lipids of membranes) and extrinsic (temperature, pH, surfactant food dyes) factors (Grey et al., 2011). In this work, Tz has been taken as an extrinsic factor to stimulate amyloid fibril formation in BLG at low pH. All the experiments were done at low pH 2.0 at room temperature. Several spectroscopic, microscopic and computational techniques were used to characterize the Tz induced amyloid fibril formation. The kinetics of amyloid fibril formation was also studied to understand the molecular mechanisms of BLG aggregation by Tz.

## 2. Materials and methods

### 2.1. Materials

Bovine beta-lactoglobulin (BLG) (lot#SLBP8394 V), Tz, glycine-HCl, and tris-HCl were purchased from Sigma Chemicals Co. (St. Louis, MO, USA). Other chemicals were consumed of analytical grade. Milli-Q water was used in the all the buffers.

### 2.2. Protein stock concentration measurements

BLG stock (6.0 mg ml<sup>-1</sup>) was made in 20 mM phosphate buffer, pH 7.4. The concentrations of BLG were calculated via Cary 60 UV-visible spectrophotometer, by measuring absorbance at 280 nm, by molar extinction coefficients 17,600 M<sup>-1</sup> cm<sup>-1</sup>.

### 2.3. Turbidity and Rayleigh scattering measurements

The turbidity and Rayleigh scattering measurements were done for the Tz treated and untreated samples by a Cary 60 UV-vis Spectrophotometer and Cary Eclipse Fluorescence Spectrofluorometer respectively. The turbidity at 650 nm and light scattering were taken at 650 nm after excitation at same wavelength. Different Tz concentrations (0.0 to 10.0 mM) were used in this study. BLG (6.0 mg ml<sup>-1</sup>) was made in 20 mM phosphate buffer at pH 7.4. Furthermore, the BLG stock was diluted almost 30.0 times in a working buffer (glycine-HCl, pH 2.0) and final concentrations of BLG was reached around 0.2 mg ml<sup>-1</sup>.

### 2.4. Kinetics of Tz-induced aggregation

The kinetics of tartrazine-induced aggregation was measured by light scattering measurements at pH 2.0. Light scattering kinetics was captured at five different conditions. All five conditions were as follows: (1) BLG at pH 2.0 (control) and BLG with 0.5 (2), 1.0

(3), and 5.0 (4) mM of Tz at pH 2.0. Tz (1.0 mM) without BLG (5) is also used as a control. The BLG concentration was fixed 0.2 mg ml<sup>-1</sup> in all the samples. The fluorescence intensity at 650 nm was recorded as a function of time (s). The excitation and emission wavelength was kept constant at 650 nm. The excitation and emission slit widths were using 1.5 nm for all the measurements.

### 2.5. Circular dichroic (CD) measurements

Far-UV CD spectra were collected on Applied Photophysics, ChirascanPlus, UK spectropolarimeter. Far-UV CD spectra were scanned with a scan speed of 100 nm/min with a response time of 2 s. Far UV-CD spectra were recorded in the wavelength range of 200–250 nm in a cuvette of 0.1 cm path length. Every sample was scanned three times and average spectra were taken. The BLG concentration was taken 0.2 mg ml<sup>-1</sup> in all the measurements. All the averaged spectra were smoothed by the Savitzky–Golay method with three convolution width. Before far-UV CD measurements, BLG was incubated with different concentrations of Tz and leave for overnight. All the incubated samples were centrifuged at 10000 rpm for 10 min to remove excess dyes. The supernatant was discarded and the precipitate was re-dissolving in the same buffer and measured the far-UV CD scan. All the CD measurements were done at room temperature.

### 2.6. Transmission electron microscopy

The morphology of Tz-induced amyloid fibrils of BLG (0.2 mg ml<sup>-1</sup>) was characterized using transmission electron microscopy (TEM). The Tz treated BLG protein samples were placed on a carbon-coated copper grid and wait for 2.0 min to proper adsorption. The sample containing grid was washed with MilliQ water and left for air-dried. The grid was negatively stained with an aqueous solution of uranyl acetate (2%, w/v) for 45 s. Excess of uranyl acetate was removed, and the samples were dried. The samples were analysed using a JOEL JEM-2100 (Japan) transmission electron microscope (TEM) operating at 200 kV. All samples images were taken at the magnification of 12,000 $\times$ .

### 2.7. Molecular docking

Autodock 4.2 was employed for elucidating the mechanism by which Tz binds to BLG by performing molecular docking as described earlier (Morris et al., 2009; Rehman et al., 2016).

#### 2.7.1. Preparation of BLG and Tz for docking

The three-dimensional coordinates of BLG were extracted from its X-ray crystal structure (PDB Id: 3NPO resolved at 2.20 Å) (Loch et al., 2011) available at RCSB database (<http://www.rcsb.org/pdb>) shown in Fig. 1A. Any heterogeneous molecule including water was removed from the structure of BLG during its preparation for molecular docking. Polar hydrogen atoms were added and the Kollman charges were assigned using AutoDock Tools (ADT). A grid of 40  $\times$  40  $\times$  40 Å dimension was created using ADT in such a way as to cover the whole active site cavity of the protein. The two-dimensional structure of Tz (CID: 164825) was retrieved from PubChem database (<https://pubchem.ncbi.nlm.nih.gov/>), and processed by adding non-polar hydrogen atoms, defining rotatable bonds, and adding Gasteiger partial charges. Finally, the energy of Tz was minimized using MMFF94 forcefield, and converted to pdbqt with the help of OpenBabel.

#### 2.7.2. Molecular docking

Lamarck Genetic Algorithm (LGA) and Solis-Wets local search protocols were used for performing molecular docking between

Tz and BLG using AutoDock 4.2 (Adeniji et al., 2020; Ali, 2019). The position, orientation, and torsion of Tz were set randomly before the start of docking procedure. A maximum of 2.5  $\times$  10<sup>6</sup> energy calculations was recorded for each run and a maximum of ten runs were performed before termination. The population size, translational step, and quaterion and torsions were set to a default value of 150, 0.2, 5, and 5 respectively. The docking results were analyzed and final figures were prepared using Discovery Studio 4.0 (Accelrys Software Inc., 2013). The binding affinity ( $K_b$ ) of Tz towards BLG was calculated from the Gibb's free energy of binding ( $\Delta G$ ) using the following relation:

$$\Delta G = -RT \ln K_b$$

where,  $R$  and  $T$  are Boltzman's universal gas constant (=1.987 cal/mol/K), and temperature (=298 K).

## 3. Results

### 3.1. Turbidity at 650 nm measurement

Turbidity measurements were carried out to investigate the impact of the Tz on BLG aggregation at pH 2.0. The turbidity at 650 nm was used to characterize the aggregation in the solutions. The graph of turbidity at 650 nm versus Tz concentrations was plotted in Fig. 2A. No turbidity was noticed in BLG at pH 2.0 indicates lowering of pH from 7 to 2 has no impact on aggregation. Increase in turbidity was recorded in the presence of 0.1 to 10.0 mM Tz. The turbidity initiated in the presence of 0.1 mM, maximum turbidity achieved at 0.8 mM, beyond 1.0 mM turbidity reaches plateau till 10.0 mM Tz. In short, an optimum concentration of Tz can induce aggregation in BLG proteins at pH 2.0. The turbidity of Tz solution (absence of BLG) was also measured but no turbidity was seen which confirm that the Tz itself not aggregating.

### 3.2. Rayleigh light scattering (RLS) measurement

The light scattering at 650 nm was exploited to reconfirm aggregation in BLG in the presence of Tz at pH 2.0. The light scattering is a good technique to measure the aggregation of proteins but has limitation to distinguish the aggregate morphology (Ismael et al., 2018, Khan et al., 2018a,b). The change in light scattering of BLG at pH 2.0 incubated with different concentration (0–10.0 mM) of Tz dye is shown in Fig. 2B. No light scattering was observed in BLG at pH 2.0, it started increasing in the presence of 0.1 mM Tz and maximized in the presence of 0.8 mM of Tz, and beyond 1.0 mM scattering was found to be plateaued. Therefore, the RLS results are supporting that ~1.0 mM Tz induces aggregation in BLG at pH 2.0. The RLS of control solution (Tz alone) was also measured to confirm that the control (Tz alone) itself is not aggregating.

### 3.3. Kinetics of Tz induced BLG aggregation

Generally, aggregation kinetics followed three steps i.e., lag phase, elongation phase and saturation phase (Michaels and Knowles, 2015). In the lag phase, the primary nucleation process starts and homogenous nuclei with highest Gibbs free energy are formed (Kumar et al., 2017). In the elongation process, the fibrils are formed not only an end-to-end attachment of protein monomers but also highly cooperative pathways i.e., secondary nucleation may take place (Rehman et al., 2016). The mature fibrils, formed at saturation phase, could considerably accelerate the rate of amyloid fibril formation, eliminate the lag time and induce immediate fibril formation (Foderà et al., 2008). The kinetics of Tz induced BLG aggregation has been monitored using light scat-

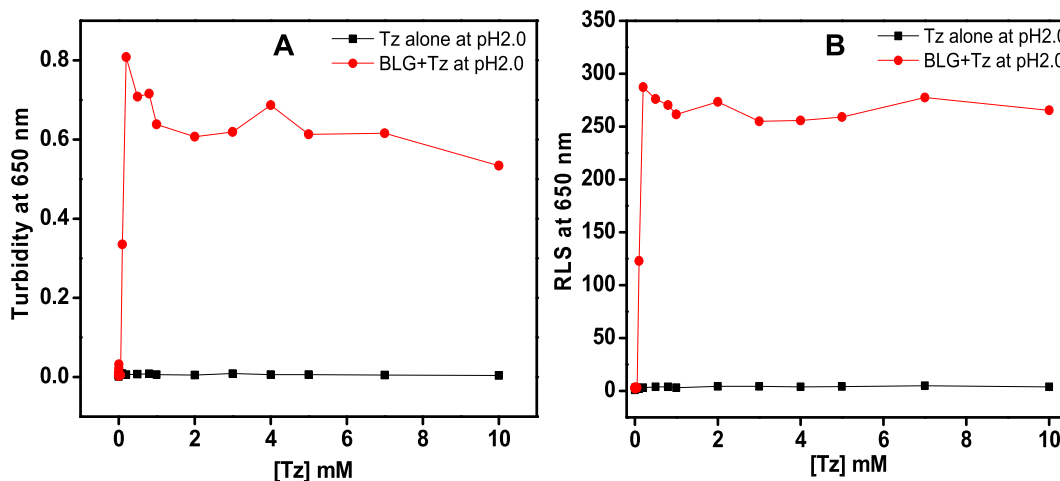


**Fig 2.** Effect of different concentrations of Tz was seen on BLG protein at pH 2.0. Turbidity (A) and light scattering (B) was measured by observing the change in absorbance (A) and light scattering (B) at 650 nm. The BLG concentration was  $0.2 \text{ mg ml}^{-1}$  in all the samples.

tering at 650 nm. It is reported that as increase in light scattering of samples occurred just because of presence of higher molecular weight species i.e., aggregates (Kong and Zeng, 2017). The kinetics of Tz-induced aggregation of BLG is shown in Fig. 3. No aggregation was observed in BLG at pH 2.0 in the absence of Tz (color) or by Tz control sample (color) within the reported time frame. However, in the presence of 0.5, 1.0 and 5.0 mM of Tz, an exponential increment in light scattering was recorded. The aggregation rate was very high and got completed within few seconds. The graph is devoid of lag phase. The absence of lag phase generally indicates aggregation without nucleation [25]. The light scattering has taken place only due to aggregation; neither BLG nor Tz has shown scattering individually. It is well reported that the length of lag phase can be altered by intrinsic (mutation) as well as extrinsic factors (salts, pH, temp and small molecules) (Kumar et al., 2014).

### 3.4. Changes in secondary structure of BLG during Tz-induced aggregation

Far-UV CD is used to monitor the changes in secondary structure of protein and peptides (Shicheng et al., 2017; Wetzel et al.,

1987). Modification in secondary structure of protein due to protein misfolding and aggregation has been identified in several neurodegenerative disorders (Arosio et al., 2015). The turbidity and light scattering data indicates that the Tz-induces aggregation in BLG protein at pH 2.0, but the changes in secondary structure were studied to understand the morphology of the aggregates. The far-UV CD spectra of native BLG and that treated with Tz samples are shown in Fig. 4, in the absence of Tz BLG shows characteristic spectrum for  $\beta$ -sheet with a single negative band at 218 nm (color), similar to the previous reports (Mecherfi et al., 2019). After addition of Tz dye, the negative ellipticity of far-UV CD spectrum was reduced and minimum at 218 nm was slightly red shifted to 220 nm. The development of new minima at 220 nm is a characteristic of cross  $\beta$ -sheet structure (Khan et al., 2016a,b). The change in percent secondary structure of BLG was calculated by K2D2. The native BLG contains almost  $29.8 \pm 0.62\%$   $\beta$ -sheet and  $20.46 \pm 0.82\%$   $\alpha$ -helix as secondary structures. No change was observed in secondary structure as pH decreased from 7.0 to 2.0. The  $\alpha$ -helicity of BLG get reduced to mere 4% and  $\beta$ -sheet increased to 49% in the presence of 0.5 mM Tz (Table 1).

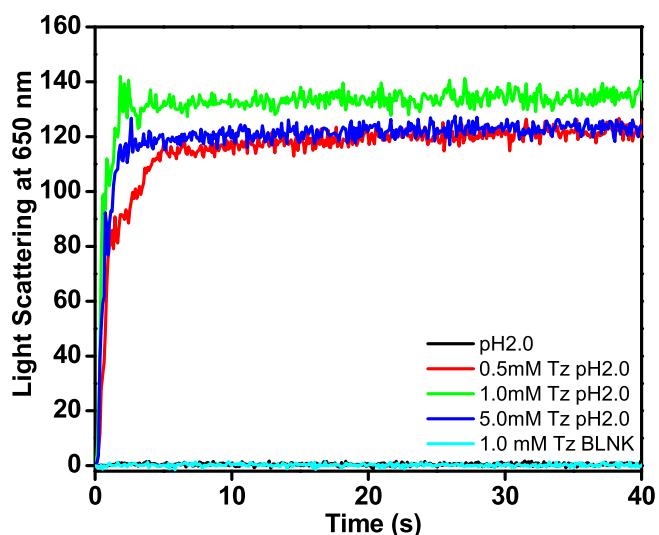


**Fig 3.** The aggregation kinetics was measured at several set of conditions including control. Light scattering at 650 nm, of  $0.2 \text{ mg ml}^{-1}$  BLG (–),  $1.0 \text{ mM}$  Tz (–), and  $0.5 \text{ mM}$  (–),  $1.0 \text{ mM}$  (–), and  $5.0 \text{ mM}$  (–) Tz with  $0.2 \text{ mg ml}^{-1}$  BLG at pH 2.0 against time (s).

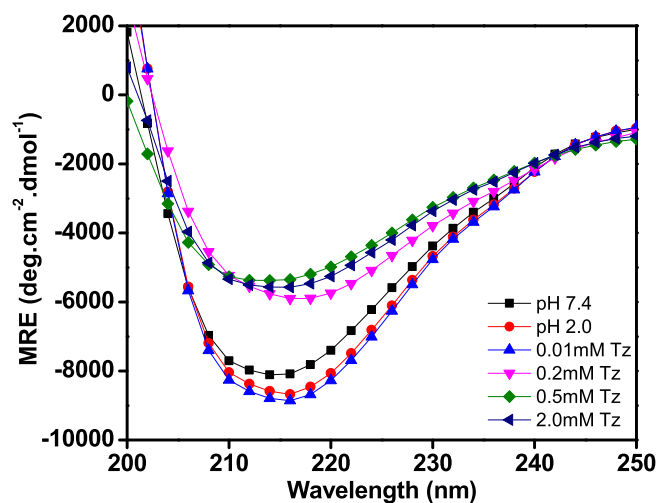


**Fig 4.** Far-UV CD spectra of BLG without Tz at pH 7.4 (–) 2.0 (–) and in the presence of different concentrations of 0.01 (–), 0.2 (–), 0.5 (–), and 2.0 (–) mM of Tz at pH 2.0. Tz treated samples were centrifuged several times at 10,000 rpm to remove excess dyes. The BLG concentrations were fixed  $0.2 \text{ mg ml}^{-1}$  in every sample.

**Table 1**  
Modification in secondary structural of BLG in response to Tz at pH 2.0.

S. No.	Conditions	Alpha-helix	Beta-sheet
1	BLG + 0.0 mM Tz at pH 7.4	20.46 ± 0.82	29.8 ± 0.62
2	BLG + 0.0 mM Tz at pH 2.0	20.46 ± 0.82	29.8 ± 0.62
3	BLG + 0.2 mM Tz at pH 2.0	6.85 ± 0.44	39.6 ± 0.80
4	BLG + 0.5 mM Tz at pH 2.0	3.8 ± 0.47	49.02 ± 0.81
5	BLG + 1.0 mM Tz at pH 2.0	8.11 ± 0.44	48.12 ± 0.99

### 3.5. TEM measurements

TEM is used to visualize the morphology of protein aggregates. To visualize the morphology of Tz-induced aggregates, TEM images of BLG at pH 2.0 were captured after incubation without and with different concentrations (0.5 and 1.0 mM) of Tz at room temperature (Fig. 5). From the figure, it is clear that the Tz-induced BLG aggregates have amyloid fibril-like morphology, similar to previous reports (Al-Shabib et al., 2017). The fibrils are unbranched, long, and straight fibrils with different diameters.

### 3.6. Molecular docking analysis

An insight into the binding mechanism of Tz with BLG and the interactions involved were identified by performing molecular docking using widely acceptable platform, Autodock. The three-

dimensional structure of BLG has shown that it harbors a deep hydrophobic cavity composed of  $\beta$ -barrels (Loch et al., 2011). This site is the primary binding site of BLG where numerous ligands have been reported to bind and interact with BLG. There are reports on the presence of two more binding sites on the surface of BLG also; however, these sites serve only as a secondary site for the binding of ligands (Ozawa et al., 2011; Liang et al., 2008). Molecular docking has been performed with Tz at the primary binding site of BLG, and the results are presented as Fig. 6A and Table 2. It seems Tz fits comfortably at the hydrophobic cavity of BLG and interaction is spontaneous ( $\Delta G^0 = -7.4$  kcal/mol). The Tz-BLG complex could be stabilized by four hydrogen bonds with Pro38 (2.39 Å), Asn109 (2.39 Å, and 2.75 Å) and Ser116 (2.08 Å) residues, and one carbon-hydrogen bond with Glu62 (3.52 Å) (Table 2). Further, an electrostatic interaction has room to get established between Tz and Lys60 (4.41 Å). The BLG-Tz complex was further stabilized by two hydrophobic interactions with Leu39 (Pi-Sigma, 3.91 Å), and Lys60 (Pi-Alkyl, 4.92 Å) that could get interrupted in highly protonated environment of pH 2.0. Other residues involved in the interaction between Tz and BLG were Leu31, Val41, Trp61, Lys69, Ile71, Asn88, Asn90, Met107, Glu108, and Leu117 (Fig. 6B). Earlier, it was found that rutin binds at the primary as well as secondary binding sites (Ozawa et al., 2011). At the primary site, rutin interacts with Leu31, Pro38, Leu39, Val41, Ile56, Leu58, Glu62, Ile84, Ala86, Leu87, Asn88, Asn90, Val92, Phe105, Met107, Ala111, Glu114, and Ser116. As it has been discussed earlier hydrogen bonding, electrostatic interactions, and

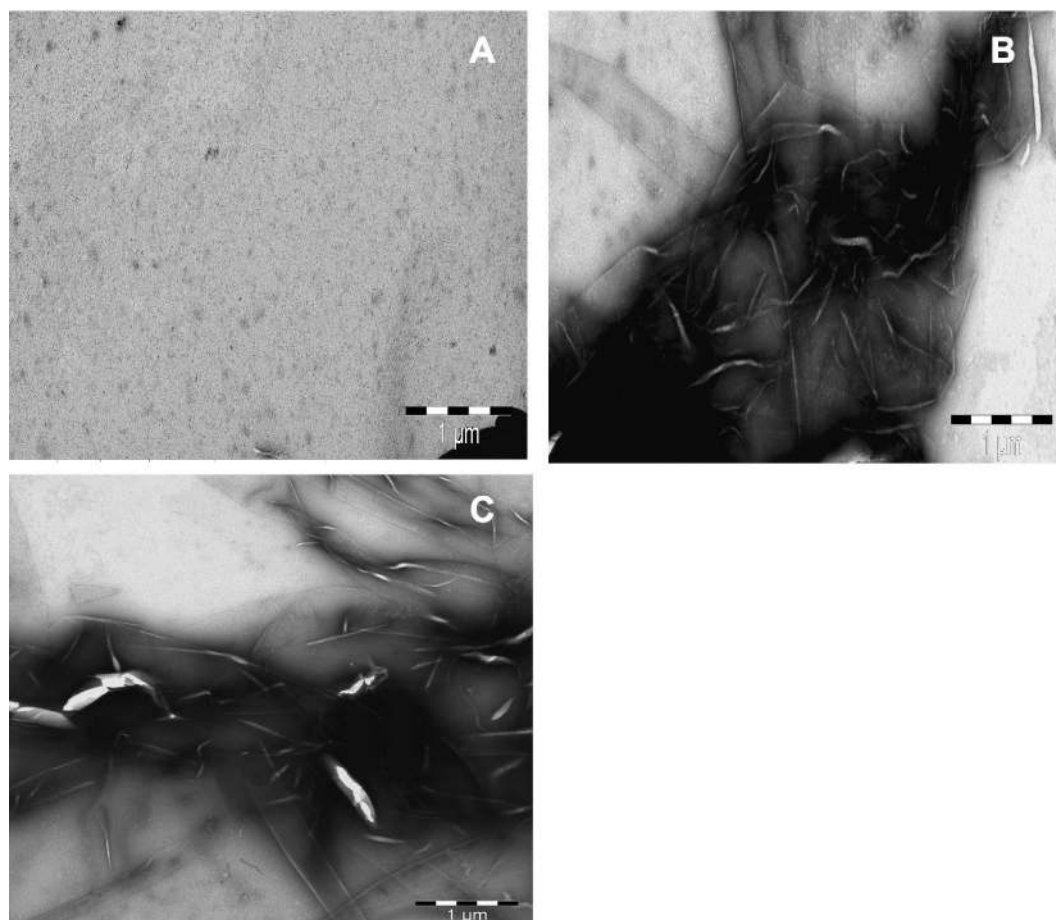


**Fig. 5.** The morphology of Tz induced amyloid fibrils of BLG protein at pH 2.0. BLG (0.2 mg ml<sup>-1</sup>) without (A), and with 0.5 mM (B) and 1.0 mM (C) of Tz treated sample.

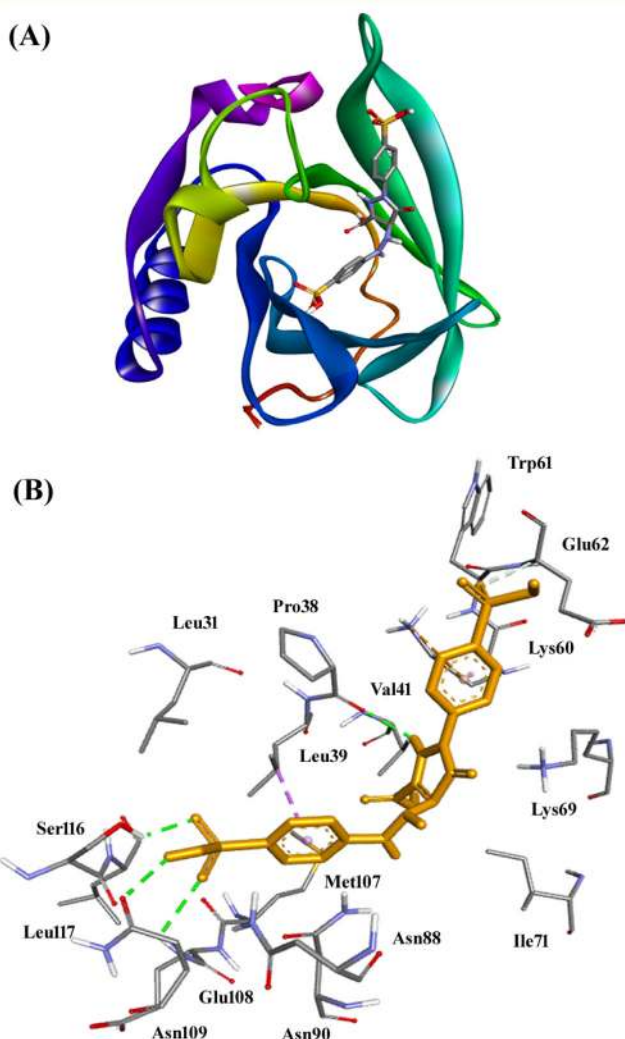


**Fig 6.** Molecular docking of Tz with BLG. Binding of Tz at the hydrophobic cavity of BLG (A), and molecular interaction involved in stabilization of the Tz and BLG complex (B).

hydrophobic interactions stabilized the Tz-BLG complex. The involvement of hydrogen bonding and hydrophobic interactions in the binding of a ligand into a hydrophobic cavity of BLG has also been previously reported (Sahihi et al., 2012). The estimated binding affinity of Tz towards BLG has been found to be  $2.67 \times 10^5 \text{ M}^{-1}$ , considerably strong binding affinity, comparable to BLG fatty acid binding.

**Table 2**

Nature of interactions	Type of bond	Distance (Å)	Binding free energy ( $\Delta G$ ), kcal/mol	Binding affinity ( $K_b$ ), $\text{M}^{-1}$
UNK1:HN – PRO38:O	Hydrogen Bond	2.39	–7.4	$2.67 \times 10^5$
UNK1:H – ASN109:OD1	Hydrogen Bond	2.39		
ASN109:HN – UNK1:O	Hydrogen Bond	2.75		
SER116:HG – UNK1:O	Hydrogen Bond	2.08		
GLU62:CA – UNK1:O	Carbon Hydrogen Bond	3.52		
LYS60:NZ – UNK1	Electrostatic (Pi-Cation)	<b>4.41</b>		
LEU39:CD1 – UNK1	Hydrophobic (Pi-Sigma)	3.91		
UNK1 – LYS60	Hydrophobic (Pi-Alkyl)	4.92		

#### 4. Discussion

Bovine  $\beta$ -lactoglobulin is a relatively small protein of 162 residues, with an 18.4 kDa. In physiological conditions it is predominantly dimeric, but dissociates to a monomer below about pH 3, preserving its native state as determined by using NMR (Uhrinova et al., 2000). Conversely,  $\beta$ -lactoglobulin also occurs in tetrameric (Timasheff and Townend, 1964) octameric (Gottschalk et al., 2003) and other multimeric (Rizzuti et al., 2010) aggregation forms under a variety of natural conditions. The secondary structure studies clearly show no change in structure from dimer (pH 7) to monomer (pH 2).

The protonated monomers of BLG at pH 2 found to start aggregating under the influence of even 0.1 mM Tz by predominantly hydrogen bonding and hydrophobic interactions and electrostatic interactions probably. In the presence of 0.5 mM Tz the aggregation completes within 3 s. A highly protonated state like pH 2.0 should support hydrogen bonding and electrostatic interaction (for Lys  $\text{pK}_a = 10.53$ ), but interrupt hydrophobic interaction. The turbidity (or RLS) observed in BLG in the presence of 0.1 mM Tz coincides with the secondary structure transition from  $\beta$ -sheet to cross  $\beta$ -sheet structure, which is a common observation during amyloid formation (Khan et al., 2016a,b). The TEM results further support the hypothesis that the fibrillation of monomeric and protonated BLG get completed even with 0.5 mM Tz.

The primary binding site of BLG is showing very good binding of Tz ( $K_d \sim 10^{-5}$ ) that is comparable with BLG affinity for fatty acids. The interaction should be spontaneous and involving hydrogen bonding and ionic interactions dominantly. Each Tz molecule has 12 hydrogen bonding acceptor chemistries. The Tz molecule could easily make bridge between BLG monomers with hydrogen bonding, but it had to compensate the cationic repulsions among BLG monomers in the process.

#### 5. Conclusions

BLG doesn't show any change from pH 7.0 to pH 2.0 and retains native like  $\beta$ -sheet structure, but forms aggregates in presence of Tz at pH 2.0. The aggregation starts even in the presence of 0.1 mM Tz. In the presence of 0.2 mM Tz, the  $\beta$ -sheet structures of BLG transform to cross  $\beta$ -sheet structures, indicating amyloid formation. The possible mechanism of Tz-induced aggregation in BLG protein is electrostatic and hydrophobic interaction because negatively charged sulphate group of tartrazine interacts electrostatically with positively charged amino acids of BLG protein and neutralizes the solvent-BLG interaction, which leads to aggregation. The participation of electrostatic and hydrophobic interactions together with hydrogen bonding is also confirmed by molecular docking. Molecular docking clearly shows that Tz binds comfortably at the hydrophobic cavity of BLG.

## Declaration of Competing Interest

The authors declare that they have no known competing financial interests or personal relationships that could have appeared to influence the work reported in this paper.

## Acknowledgments

The authors extend their appreciation to Deanship of Scientific Research at King Saud University for funding this work through Research Group no. RGP-1439-014.

## References

- Abelein, A., Kaspersen, J.D., Nielsen, S.B., Jensen, G.V., Christiansen, G., Pedersen, J.S., Danielsson, J., Otzen, D.E., Gräslund, A., 2013. Formation of dynamic soluble surfactant-induced amyloid  $\beta$  peptide aggregation intermediates. *J. Biol. Chem.* 288 (32), 23518–23528.
- Adeniji, S.E., Uba, S., Uzairu, A., 2020. In silico study for evaluating the binding mode and interaction of 1,2,4-triazole and its derivatives as potent inhibitors against Lipotease protein B (LipB). *J. King Saud Univ. – Sci.* 32 (1), 475–485.
- Ali, M.A., 2019. Molecular docking and molecular dynamics simulation of anticancer active ligand '3,5,7,3',5'-pentahydroxy-flavanonol-3-O- $\alpha$ -L-rhamnopyranoside' from *Bauhinia strychnifolia* Craib to the cyclin-dependent protein kinase. *J. King Saud Univ. Sci.* (in press).
- Al-Shabib, N.A., Khan, J.M., Khan, M.S., Ali, M.S., Al-Senaidey, A.M., Alsenaidy, M.A., Husain, F.M., Al-Lohedan, H.A., 2017. Synthetic food additive dye "Tartrazine" triggers amorphous aggregation in cationic myoglobin. *Int. J. Biol. Macromol.* 98, 277–286.
- Arosio, P., Knowles, T.P., Linse, S., 2015. On the lag phase in amyloid fibril formation. *Phys. Chem. Chem. Phys.* 17 (12), 7606–7618.
- Biancalana, M., Koide, S., 2010. Molecular mechanism of Thioflavin-T binding to amyloid fibrils. *Biochim. Biophys. Acta* 1804 (7), 1405–1412.
- Bieler, S., Estrada, L., Lagos, R., Baeza, M., Castilla, J., Soto, C., 2005. Amyloid formation modulates the biological activity of a bacterial protein. *J. Biol. Chem.* 280 (29), 26880–26885.
- Blancas-Mejia, L.M., Ramirez-Alvarado, M., 2013. Systemic amyloidosis. *Annu. Rev. Biochem.* 82, 745–774.
- Chiti, F., Dobson, C.M., 2017. Protein misfolding, amyloid formation, and human disease: a summary of progress over the last decade. *Annu. Rev. Biochem.* 86, 27–68.
- Chiti, F., Webster, P., Taddei, N., Clark, A., Stefani, M., Ramponi, G., Dobson, C.M., 1999. Designing conditions for *in vitro* formation of amyloid protofilaments and fibrils. *Proc. Natl. Acad. Sci. USA* 96 (7), 3590–3594.
- Collins, T.F., Black, T.N., Brown, L.H., Bulhac, P., 1990. Study of the teratogenic potential of FD & C yellow No. 5 when given by gavage to rats. *Food Chem. Toxicol.* 28 (12), 821–827.
- Eman, G.E., Samir, A.M., Hamdy, A., 2000. Effects of some food colorants (synthetic and natural products) of young albino rats. *Egypt. J. Hosp. Med.* 1, 103–113.
- Foderà, V., Librizzi, F., Groenning, M., Van de Weert, M., Leone, M., 2008. Secondary nucleation and accessible surface in insulin amyloid fibril formation. *J. Phys. Chem. B* 112 (12), 3853–3858.
- Gottschalk, M., Nilsson, H., Roos, H., Halle, B., 2003. Protein self-association in solution: The bovine  $\beta$ -lactoglobulin dimer and octamer. *Protein Sci.* 12, 2404–2411.
- Grey, M., Linse, S., Nilsson, H., Brundin, P., Sparr, E., 2011. Membrane interaction of  $\alpha$ -synuclein in different aggregation states. *J. Parkinsons Dis.* 1 (4), 359–371.
- Hofer, K., Jenewein, D., 1997. Quick spectrophotometric identification of synthetic food colorants by linear regression analysis. *Food Res. Technol.* 204, 32–38.
- Ismael, M.A., Khan, J.M., Malik, A., Alsenaidy, M.A., Hidayathulla, S., Khan, R.H., Sen, P., Irfan, M., Alsenaidy, A.M., 2018. Unraveling the molecular mechanism of the effects of sodium dodecyl sulfate, salts, and sugars on amyloid fibril formation in camel IgG. *Colloids Surf. B Biointerfaces* 170, 430–437.
- Khan, J.M., Khan, M.S., Ali, M.S., AlShabib, N.A., Khan, R.H., 2016a. Cetyltrimethylammonium bromide (CTAB) promote amyloid fibril formation in carbohydrate binding protein (concanavalin A) at physiological pH. *RSC Adv.* 6, 38100–38111.
- Khan, J.M., Khan, M.S., Alsenaidy, M.A., Ahmed, A., Sen, P., Oves, M., Al-Shabib, N.A., Khan, R.H., 2018a. Sodium lauryl sarcosinate (sarkosyl) modulate amyloid fibril formation in hen egg white lysozyme (HEWL) at alkaline pH: a molecular insight study. *J. Biomol. Struct. Dyn.* 36 (6), 1550–1565.
- Khan, J.M., Sharma, P., Arora, K., Kishor, N., Kaila, P., Guptasarma, P., 2016b. The Achilles' Heel of "Ultrastable" hyperthermophile proteins: submillimolar concentrations of SDS stimulate rapid conformational change, aggregation, and amyloid formation in proteins carrying overall positive charge. *Biochemistry* 55 (28), 3920–3936.
- Khan, M.V., Zaman, M., Chandel, T.I., Siddiqui, M.K., Ajmal, M.R., Abdelhameed, A.S., Khan, R.H., 2018b. Cationic surfactant mediated fibrillogenesis in bovine liver catalase: a biophysical approach. *J. Biomol. Struct. Dyn.* 36 (10), 2543–2557.
- Kong, L.X., Zeng, C.M., 2017. Effects of seeding on lysozyme amyloid fibrillation in the presence of epigallocatechin and polyethylene glycol. *Biochemistry (Mosc)* 82, 156–167.
- Kumar, E.K., Haque, N., Prabhu, N.P., 2017. Kinetics of protein fibril formation: Methods and mechanisms. *Int. J. Biol. Macromol.* 100, 3–10.
- Kumar, S., Tepper, K., Kaniyappan, S., Biernat, J., Wegmann, S., Mandelkow, E.M., Müller, D.J., Mandelkow, E., 2014. Stages and conformations of the Tau repeat domain during aggregation and its effect on neuronal toxicity. *J. Biol. Chem.* 289, 20318–20332.
- Liang, L., Tajmir-Riahi, H.A., Subirade, M., 2008. Interaction of beta-lactoglobulin with resveratrol and its biological implications. *Biomacromolecules* 9 (1), 50–56.
- Loch, J., Polit, A., Gorecki, A., Bonarek, P., Kurpiewska, K., Dziejicka-Wasyulewska, M., Lewinski, K., 2011. Two modes of fatty acid binding to bovine beta-lactoglobulin-crystallographic and spectroscopic studies. *J. Mol. Recognit.* 24, 341–349.
- Mecherfi, K.E.E.1., Curet, S., Roberta, L., Larre, C., Rouaud, O., Choiset, Y., Rabesona, H., Haertle, T., 2019. Combined microwave processing and enzymatic proteolysis of bovine whey proteins: the impact on bovine  $\beta$ -lactoglobulin allergenicity. *J. Food Sci. Technol.* 56, 177–186.
- Merinas-Amo, R., Martínez-Jurado, M., Jurado-Güeto, S., Alonso-Moraga, Á., Merinas-Amo, T., 2019. Biological effects of food coloring in vivo and in vitro model system. *Foods* 8 (5), 176.
- Michaels, T.C.T., Knowles, T.P.J., 2015. Kinetic theory of protein filament growth: Self-consistent methods and perturbative techniques. *Int. J. Mod. Phys. B* 29, 1530002–1530023.
- Morris, G.M., Huey, R., Lindstrom, W., Sanner, M.F., Belew, R.K., Goodsell, D.S., Olson, A.J., 2009. Autodock4 and AutoDockTools4: automated docking with selective receptor flexibility. *J. Comput. Chem.* 16, 2785–2791.
- Ozawa, D., Hasegawa, K., Lee, Y.H., Sakurai, K., Yanagi, K., Ookoshi, T., Goto, Y., Naiki, H., 2011. Inhibition of beta2-microglobulin amyloid fibril formation by alpha2-macroglobulin. *J. Biol. Chem.* 286 (11), 9668–9676.
- Poul, M., Jarry, G., Elhkim, M.O., Poul, J.M., 2009. Lack of genotoxic effect of food dyes amaranth, sunset yellow and tartrazine and their metabolites in the gut micronucleus assay in mice. *Food Chem. Toxicol.* 47 (2), 443–448.
- Rehman, M.T., Ahmed, S., Khan, A.U., 2016. Interaction of meropenem with 'N' and 'B' isoforms of human serum albumin: a spectroscopic and molecular docking study. *J. Biomol. Struct. Dyn.* 34 (9), 1849–1864.
- Rizzuti, B., Zappone, B., De Santo, M.P., Guzzi, R., 2010. Native  $\beta$ -lactoglobulin self-assembles into a hexagonal columnar phase on a solid surface. *Langmuir* 26, 1090–1095.
- Sahihi, M., Heidari-Koholi, Z., Bordbar, A.K., 2012. The interaction of polyphenol flavonoids with  $\beta$ -lactoglobulin: molecular docking and molecular dynamics simulation studies. *J. Macromol. Sci. B* 51 (12), 2311–2323.
- Schmitt, C., Bovay, C., Rouvet, M., Shojaei-Rami, S., Kolodziejczyk, E., 2007. Whey protein soluble aggregates from heating with NaCl: physicochemical, interfacial, and foaming properties. *Langmuir* 23, 4155–4166.
- Shicheng, L., Donglan, X., Muhammad, S., Asad, R., Xiaoxiong, Z., 2017. Characterization of molecular structures of theaflavins and the interactions with bovine serum albumin. *J. Food Sci. Technol. Mys.* 54, 3421–3432.
- Shirahama, T., Cohen, A.S., 1996. High resolution electron microscopic analysis of the amyloid fibril. *J. Cell Biol.* 33, 679–706.
- Tanaka, T., Takahashi, O., Oishi, S., Ogata, A., 2008. Effects of tartrazine on exploratory behavior in a three-generation toxicity study in mice. *Reprod. Toxicol.* 26 (2), 156–163.
- Timasheff, S.N., Townsend, R., 1964. Structure of the  $\beta$ -lactoglobulin tetramer. *Nature* 203, 517–519.
- Uhrinova, S., Smith, M.H., Jameson, G.B., Uhrin, D., Sawyer, L., Barlow, P.N., 2000. Structural changes accompanying pH-induced dissociation of the beta-lactoglobulin dimer. *Biochemistry* 39, 3565–3574.
- Verheul, M., Pedersen, J.S., Roefs, S.P.F.M., De Kruijff, C.G., 1999. Association behavior of native  $\alpha$ -lactoglobulin. *Biopolymers* 49, 11–20.
- Wawer, J., Szociński, M., Olszewski, M., Piątek, R., Naczka, M., Krakowiak, J., 2018. Influence of the ionic strength on the amyloid fibrillogenesis of hen egg white lysozyme. *Int. J. Biol. Macromol.* 121, 63–70.
- Wetzel, R., Buder, E., Hermel, H., Hiittner, A., 1987. Conformations of different gelatins in solutions and in films an analysis of circular dichroism (CD) measurements. *Colloid Polym. Sci.* 265, 1036–1045.